

Functional Impact of the Ryanodine Receptor on the Skeletal Muscle L-Type Ca^{2+} Channel

Guillermo Avila and Robert T. Dirksen

From the Department of Pharmacology and Physiology, University of Rochester School of Medicine and Dentistry, Rochester, New York 14642

abstract L-type Ca^{2+} channel (L-channel) activity of the skeletal muscle dihydropyridine receptor is markedly enhanced by the skeletal muscle isoform of the ryanodine receptor (RyR1) (Nakai, J., R.T. Dirksen, H.T. Nguyen, I.N. Pessah, K.G. Beam, and P.D. Allen. 1996. *Nature*. 380:72–75.). However, the dependence of the biophysical and pharmacological properties of skeletal L-current on RyR1 has yet to be fully elucidated. Thus, we have evaluated the influence of RyR1 on the properties of macroscopic L-currents and intracellular charge movements in cultured skeletal myotubes derived from normal and “RyR1-knockout” (dyspedic) mice. Compared with normal myotubes, dyspedic myotubes exhibited a 40% reduction in the amount of maximal immobilization-resistant charge movement (Q_{max} , 7.5 ± 0.8 and 4.5 ± 0.4 nC/ μF for normal and dyspedic myotubes, respectively) and an approximately fivefold reduction in the ratio of maximal L-channel conductance to charge movement ($G_{\text{max}}/Q_{\text{max}}$). Thus, RyR1 enhances both the expression level and Ca^{2+} conducting activity of the skeletal L-channel. For both normal and dyspedic myotubes, the sum of two exponentials was required to fit L-current activation and resulted in extraction of the amplitudes (A_{fast} and A_{slow}) and time constants (τ_{slow} and τ_{fast}) for each component of the macroscopic current. In spite of a >10-fold in difference current density, L-currents in normal and dyspedic myotubes exhibited similar relative contributions of fast and slow components (at +40 mV; $A_{\text{fast}}/[A_{\text{fast}} + A_{\text{slow}}] \sim 0.25$). However, both τ_{fast} and τ_{slow} were significantly ($P < 0.02$) faster for myotubes lacking the RyR1 protein (τ_{fast} , 8.5 ± 1.2 and 4.4 ± 0.5 ms; τ_{slow} , 79.5 ± 10.5 and 34.6 ± 3.7 ms at +40 mV for normal and dyspedic myotubes, respectively). In both normal and dyspedic myotubes, (–) Bay K 8644 (5 μM) caused a hyperpolarizing shift (~ 10 mV) in the voltage dependence of channel activation and an 80% increase in peak L-current. However, the increase in peak L-current correlated with moderate increases in both A_{slow} and A_{fast} in normal myotubes, but a large increase in only A_{fast} in dyspedic myotubes. Equimolar substitution of Ba^{2+} for extracellular Ca^{2+} increased both A_{fast} and A_{slow} in normal myotubes. The identical substitution in dyspedic myotubes failed to significantly alter the magnitude of either A_{fast} or A_{slow} . These results demonstrate that RyR1 influences essential properties of skeletal L-channels (expression level, activation kinetics, modulation by dihydropyridine agonist, and divalent conductance) and supports the notion that RyR1 acts as an important allosteric modulator of the skeletal L-channel, analogous to that of a Ca^{2+} channel accessory subunit.

key words: excitation–contraction coupling • skeletal muscle • charge movement

INTRODUCTION

Skeletal and cardiac muscle dihydropyridine receptors (DHPRs)¹ are voltage-dependent L-type calcium channels (L-channels) (Tanabe et al., 1988; Mikami et al., 1989) that control the activity of intracellular Ca^{2+} release channels, ryanodine receptors (RyRs), during excitation–contraction (EC) coupling (McPherson and Campbell, 1993). In cardiac muscle, the release of intracellular Ca^{2+} from the sarcoplasmic reticulum (SR)

depends on the influx of extracellular calcium through cardiac DHPRs (Nabauer et al., 1989). However, influx of extracellular calcium through voltage-gated Ca^{2+} channels is not a requirement for SR Ca^{2+} release or contraction in skeletal muscle (Armstrong et al., 1972; Garcia and Beam, 1994; Dirksen and Beam, 1999). Rather, EC coupling in skeletal muscle is thought to involve a mechanical interaction between sarcolemmal DHPRs and the skeletal muscle RyR isoform (RyR1) (Schneider and Chandler, 1973). During EC coupling in skeletal muscle, the DHPRs undergo voltage-driven conformational changes that result in the activation of SR Ca^{2+} release channels (“orthograde signal”). Thus, the DHPR in skeletal muscle functions as both a voltage sensor for EC coupling (Ríos and Brum, 1987) and as a voltage-gated L-channel (Tanabe et al., 1988).

Interestingly, the presence of the RyR1 protein promotes the Ca^{2+} conducting activity and accelerates the

Portions of this work were previously published in abstract form (Avila, G., and R.T. Dirksen. 2000. *Biophys. J.* 78:427a).

Address correspondence to Robert T. Dirksen, Department of Pharmacology and Physiology, University of Rochester School of Medicine and Dentistry, 601 Elmwood Avenue, Rochester, NY 14642. Fax: 716-273-2652; E-mail: robert_dirksen@urmc.rochester.edu

¹Abbreviations used in this paper: DHPR, dihydropyridine receptor; EC, excitation–contraction; L-channel, L-type Ca^{2+} channel; RyR, ryanodine receptor; SR, sarcoplasmic reticulum.

activation of skeletal L-channels ("retrograde signal") (Fleig et al., 1996; Nakai et al., 1996). This finding was based, in part, on experiments involving cultured skeletal myotubes derived from mice homozygous for a disrupted RyR1 gene (RyR1-knockout or dyspedic mice; Takeshima et al., 1994; Nakai et al., 1996). Compared with normal myotubes, dyspedic myotubes exhibit a dramatic reduction in the density of L-current (Fleig et al., 1996; Nakai et al., 1996). Moreover, expression of RyR1 in dyspedic myotubes enhances L-current in the absence of a change in intramembrane charge movement (Nakai et al., 1996). These observations led to the conclusion that RyR1 promotes the Ca²⁺ channel activity of the skeletal muscle DHPR in a manner that is independent of L-channel expression. Moreover, this ability seems to be a unique property of RyR1 since the cardiac isoform (RyR2) is incapable of restoring either EC coupling or robust skeletal L-currents in dyspedic myotubes (Nakai et al., 1997). Thus, the signaling between the skeletal muscle DHPR and RyR1 is bidirectional, such that the channel activity associated with each protein is strongly dependent upon this unique interaction.

Interaction between intracellular signaling molecules, such as G-proteins (for review, see Dolphin, 1998) and proteins of the synaptic core complex (SNARE proteins) (for review, see Catterall, 1999), markedly alter the functional properties of voltage-dependent Ca²⁺ channels. Thus, the reciprocal nature of the interaction between the DHPR and RyR in skeletal muscle appears to represent an additional example of a voltage-gated Ca²⁺ channel that is functionally modulated by interaction with an intracellular signaling partner. The orthograde and retrograde signals of skeletal muscle EC coupling appear to be mediated by the intracellular loop that links the second and third internal homology repeats (II-III loop) of the skeletal muscle DHPR (Tanabe et al., 1990; Nakai et al., 1998a; Grabner et al., 1999). However, results from the expression of chimeric RyRs into dyspedic myotubes indicate that these two signals are localized to distinct regions within RyR1 (Nakai et al., 1998b). Thus, although dyspedic myotubes provide an excellent model for probing structure/function relationships of RyR1 on skeletal muscle EC coupling, the precise influence of RyR1 on the fundamental properties of skeletal L-channels has yet to be fully elucidated. Here, we describe experiments designed to characterize the influence of the RyR1 protein on the biophysical and pharmacological properties of the skeletal L-channel. Our data demonstrates that L-currents recorded from normal and dyspedic myotubes exhibit two distinct kinetic components that are equivalently enhanced by RyR1. In addition, our results indicate that RyR1 influences L-channel expression, activation kinetics, modulation by DHP agonists, and divalent conductance.

METHODS

Preparation of Normal and Dyspedic Myotubes

Primary cultures of myotubes were prepared from skeletal muscle of newborn normal and dyspedic mice as described previously (Nakai et al., 1996). The presence (or absence) of RyR1 mutant alleles was determined by PCR analysis on tail snip tissue obtained from each animal used to generate cultures. Thus, each individual culture was identified as homozygous normal (+/+), heterozygous normal (+/-), or dyspedic (-/-). Data obtained from homozygous and heterozygous normal cultures were ultimately pooled together since no significant differences in macroscopic L-channel activity were observed between all normal myotubes (see Table I). Expression of RyR1 in dyspedic myotubes was performed as previously described (Dirksen and Beam, 1999). In brief, myotubes were microinjected (Tanabe et al., 1988) into a single nucleus with wild-type RyR1 cDNA (0.5 µg/µl) 6–8 d after the initial plating of myoblasts and were examined electrophysiologically 2–4 d later. Expressing myotubes were identified by observing contractions in response to external electrical stimulation (8.0 V, 10–30 ms). In some experiments, expressing myotubes were identified by the development of green fluorescence 2–4 d after coinjection with a mixture of RyR1 cDNA (0.5 µg/µl) and a cDNA expression plasmid encoding an enhanced green fluorescent protein (0.01 µg/µl) (Grabner et al., 1999).

Electrophysiologic Measurements

Whole-cell patch-clamp experiments were carried out at room temperature (20–22°C), 7–11 d after the initial plating of myoblasts. For all experiments, the holding potential was –80 mV. T-type Ca²⁺ currents were eliminated by a conditioning prepulse consisting of a 1-s depolarization to –20 mV followed by a 25-ms repolarization to –50 mV before each test pulse (Adams et al., 1990; Dirksen and Beam, 1999). Currents were recorded with either a Dagan 3900A (Dagan Corp.) or Axopatch 200A (Axon Instruments Inc.) amplifier and filtered at 2 kHz by a four-pole Bessel filter. Data were digitized at 10 kHz using a DigiData 1200 interface (Axon Instruments, Inc.) and analyzed using the pCLAMP (Axon Instruments, Inc.) and SigmaPlot (SPSS Inc.) software suites. Capacitative currents were minimized (>90%) using the capacitative transient cancellation feature of the amplifier. The remaining linear components were subtracted using a P/3 leak subtraction protocol. Cell capacitance (C_m) was determined by integration of the capacity transient resulting from a +10-mV pulse applied from the holding potential and was used to normalize ionic (pA/pF) and gating (nC/µF) currents obtained from different myotubes. Relatively large dyspedic myotubes were used to compensate for the relatively L-current density (~1.0 pA/pF) found in these cells. C_m values were (pF): 322 ± 27 (n = 44), 607 ± 55 (n = 38), and 454 ± 33 (n = 82), for normal myotubes, dyspedic myotubes, and all experiments, respectively. The average series (access) resistance (R_s) after compensation was 1.1 ± 0.07 MΩ (n = 82), and the voltage error due to series resistance (V_e = R_s × I_{Ca}) was less than ~5 mV (for these experiments, the average was 2.66 ± 0.19 mV, n = 82). The average time constant for charging the membrane capacitance (τ_m = R_s × C_m) was 0.37 ± 0.02 ms (n = 82) and was never larger than 1.21 ms. All data are presented as mean ± SEM.

Macroscopic Calcium Currents

The whole-cell variant of the patch clamp technique (Hamill et al., 1981) was used to compare the properties of macroscopic L-currents of normal myotubes, uninjected dyspedic myotubes, and dyspedic myotubes injected with cDNA encoding the wild-

type rabbit RyR1. Patch pipettes were fabricated from borosilicate glass and had resistances of 1.5–2.0 M Ω when filled with internal solution (see below). Peak inward Ca²⁺ currents were assessed at the end of 200-ms test pulses of variable amplitude and plotted as a function of the membrane potential (I-V curves). I-V curves were subsequently fitted according to:

$$I = G_{\max}(V - V_{\text{rev}}) / \{1 + \exp[(V_{G1/2} - V) / k_G]\}, \quad (1)$$

where V_{rev} is the extrapolated reversal potential of the calcium or barium current, V is the membrane potential during the test pulse, I is the peak current during the test pulse, G_{\max} is the maximum L-channels conductance, $V_{G1/2}$ is the voltage for half activation of G_{\max} , and k_G is the slope factor. The activation phase of macroscopic ionic currents was fitted using one of the following exponential functions (Eqs. 2 and 3):

$$I(t) = A_0[\exp(-t/\tau_0)] + C \quad (2)$$

$$I(t) = A_{\text{fast}}[\exp(-t/\tau_{\text{fast}})] + A_{\text{slow}}[\exp(-t/\tau_{\text{slow}})] + C, \quad (3)$$

where $I(t)$ is the current at time t after the depolarization, A_0 , A_{fast} , and A_{slow} are the steady state current amplitudes of each component with their respective time constants of activation (τ_0 , τ_{fast} , and τ_{slow}), and C represents the steady state peak current. In all cases, the fitting procedure started at the zero current level, which corresponded to 5–7 ms after the initiation of the voltage pulse ($>10 \times \tau_m$). This approach limited artifacts introduced by the declining phase of Q_{on} , since the magnitude of Q_{on} reaches $>90\%$ of its maximal value before this time (see Fig. 1). In addition, L-currents were also recorded before and after ionic current blockade with 0.5 mM Cd²⁺ + 0.2 mM La³⁺ in a separate set of experiments. The Cd²⁺/La³⁺-sensitive currents lacked intramembrane charge movements and exhibited nearly identical activation kinetics as those obtained before gating current subtraction (data not shown). Thus, the fast component of L-current activation described in this study is not greatly influenced by the declining phase of the Q_{on} gating current transient.

Intramembrane Charge Movement

Immobilization-resistant intramembrane charge movements were measured in whole-cell mode by a method described previously (Adams et al., 1990). Calcium currents were blocked by the addition of 0.5 mM CdCl₂ + 0.2 mM LaCl₃ to the extracellular recording solution. This combination of Cd²⁺ and La³⁺ effectively blocks ionic calcium currents carried through calcium channels in normal myotubes (Adams et al., 1990; Garcia and Beam, 1994; Dirksen and Beam, 1995). To prevent amplifier saturation, voltage clamp command pulses were exponentially rounded with a time constant of 240 μ s. The amount of immobilization-resistant charge movement was estimated by integrating the transient of charge that moved outward after the onset of the test pulse (Q_{on}). The magnitude of the maximum immobilization-resistant charge movement (Q_{\max}) was estimated by fitting the Q_{on} data according to:

$$Q_{\text{on}} = Q_{\max} / \{1 + \exp[(V_{Q1/2} - V) / k_Q]\}, \quad (4)$$

where $V_{Q1/2}$ and k_Q have their usual meanings with regard to charge movement.

Recording Solutions

For measurements of macroscopic ionic and gating currents, the internal solution consisted of (mM): 140 Cs-aspartate, 10 Cs₂-

EGTA, 5 MgCl₂, and 10 HEPES, pH 7.40 with CsOH. Macroscopic calcium currents were recorded in an external solution containing (mM): 145 TEA-Cl, 10 CaCl₂, 0.003 TTX (Alomone Laboratories), and 10 HEPES, pH 7.40 with TEA-OH. For measurements of macroscopic barium currents, 10 mM BaCl₂ was substituted for the 10 mM CaCl₂ in the external solution. The external calcium current recording solution was supplemented with 0.5 mM CdCl₂ + 0.2 mM LaCl₃ for measurements of intramembrane charge movement. For some experiments, the influence of RyR1 on the stimulatory action of (–) Bay K 8644 (0.005 mM), a pure DHP agonist, was evaluated after addition to the external calcium current recording solution. Except where noted, all chemical reagents were obtained from Sigma Chemical Co.

RESULTS

Dyspedic Myotubes Exhibit a Reduction in Immobilization-resistant Charge Movement

If the gating charge moved is similar for channels with different P_o s, then the density of channel proteins can be estimated from the magnitude of the maximal immobilization-resistant intramembrane charge movement (Q_{\max}) (Adams et al., 1990; Nakai et al., 1996). The values of Q_{\max} reported for normal myotubes originating from the dysgenic line of mice (which lack a functional copy of the skeletal DHPR gene) have varied (nC/ μ F): 7.9 ± 1.4 (Adams et al., 1990), 7.2 ± 0.5 (Dirksen and Beam, 1995), 5.6 ± 2.6 (Nakai et al., 1996), and 5.1 ± 0.9 (Garcia et al., 1994). This variability, coupled with the fact that the dyspedic mice were constructed from a separate mouse lineage, prompted us to compare the magnitude of Q_{\max} in dyspedic myotubes with myotubes derived from their phenotypically normal littermates (normal myotubes). The voltage dependence of the charge movement obtained from these experiments is illustrated in Fig. 1. On average, the Q_{\max} values of normal and dyspedic myotubes were 7.5 ± 0.8 ($n = 17$) and 4.5 ± 0.4 ($n = 14$) nC/ μ F, respectively. Thus, dyspedic myotubes exhibit a 40% reduction in Q_{\max} compared with the magnitude of Q_{\max} obtained from normal myotubes derived from their phenotypically normal littermates. This 40% reduction in the magnitude of Q_{\max} in dyspedic myotubes is quantitatively similar to previous studies that reported a reduction in total DHP binding in dyspedic muscle (25%, Fleig et al., 1996; 50%, Buck et al., 1997). Interestingly, the $V_{Q1/2}$ of Q_{on} in dyspedic myotubes was ~ 10 mV more hyperpolarized than that of normal myotubes (Fig. 1 C and Table I). Thus, the RyR1 protein not only promotes the long-term functional expression of DHPRs, but also modifies the voltage sensitivity of DHPR's mediated gating currents. The difference in DHPR's gating current sensitivity to activation by voltage (i.e., $V_{Q1/2}$) was reversed 2–4 d after nuclear injection of dyspedic myotubes with cDNA encoding wild-type RyR1 (Fig. 1 C and Table I). However, the restoration of Q_{on} voltage sensitivity by RyR1 expression in dyspedic myotubes occurred in the absence of an effect on Q_{\max} (see

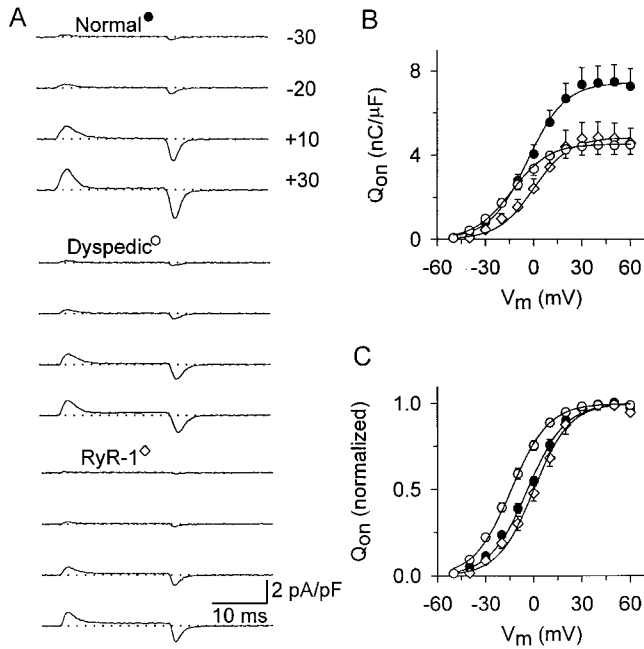


Figure 1. Voltage dependence of charge movements. (A) Intradepolarization charge movements recorded from normal (top), dyspedic (middle), and RyR1-expressing dyspedic (bottom) myotubes. The recordings for each data set were elicited by 20-ms depolarizations to the indicated voltages (mV). (B) Average voltage dependence of charge movements (Q_{on}) obtained from 17 normal (●), 14 dyspedic (○) and 7 RyR1-expressing dyspedic (◇) myotubes. Values of Q_{on} were determined by integrating the “on” outward transient at each membrane potential and normalized to cell capacitance (C_m). The average values (\pm SEM) for the parameters obtained by fitting each myotube within a group separately to Eq. 4 are given in Table I. The smooth solid lines through the data were generated by using Eq. 4 and the average values (Q - V) given in Table I. (C) The Q_{on} values from B were normalized to their maximal value and plotted versus V_m .

also Nakai et al., 1996), suggesting that the restoration of a “normal” level of Q_{max} may reflect a slower process involving protein synthesis and/or membrane trafficking.

Null mutations of a single allele in a diploid organism could potentially result in a reduced probability of gene expression, and thus lead to haploinsufficiency. Therefore, we have investigated whether the presence of a single wild-type RyR1 allele is sufficient to supply the number of ryanodine receptors required to sustain normal L-channel activity. With this in mind, normal myotubes were genotyped and divided into two groups: homozygous normal (+/+) and heterozygous normal (+/-) for the wild-type RyR1 allele. However, no significant ($P > 0.4$) differences were found in the voltage-dependent parameters of either L-channel conductance or charge movement (Table I) between these two genotypic groups. These data are in agreement with morphological studies that indicate that muscle fibers obtained from homozygous and heterozygous normal embryos are structurally indistinguishable (Takekura et al., 1995). Thus, data from homozygous and heterozygous normal myotubes were pooled together in all subsequent analyses.

Dyspedic myotubes exhibit a very modest amount of slowly activating L-current, which is greatly enhanced 2–4 d after nuclear injection of wild-type RyR1 cDNA (Nakai et al., 1996; Fig 2, A and B). In our experiments, the average peak L-currents were (at +30 mV) (pA/pF): 12.1 ± 0.6 ($n = 27$), 1.1 ± 0.4 ($n = 9$), and 8.4 ± 0.6 ($n = 6$) for normal, dyspedic, and RyR1-expressing dyspedic myotubes, respectively. Since normal myotubes exhibit a larger Q_{max} compared with uninjected and RyR1-expressing dyspedic myotubes (Fig. 1 and Table I), we normalized peak L-current data by the Q_{max} value for each myotube (current-to-charge ratio). The normalized data (Fig. 2 C) demonstrates that expression of RyR1 in dyspedic myotubes restores the current-to-charge ratio at every potential and suggests that equivalent fractions of L-channels are upregulated in normal

TABLE I
Parameters of Fitted I-V and Q-V Curves

	<i>n</i>		I-V data			Q-V data				
	I-V	Q-V	G_{max}	$V_{G1/2}$	k_G	Q_{max}	$V_{Q1/2}$	k_Q	G_{max}/Q_{max}	
			nS/nF	mV	mV	nC/ μ F	mV	mV	nS/pC	
(+/+)	13	10	250 ± 19	13.7 ± 1.0	5.1 ± 0.2	8.1 ± 1.1	-3.1 ± 0.9	11.6 ± 0.5	35.1 ± 3.7	(10)
(+/-)	14	7	245 ± 12	11.7 ± 1.0	5.7 ± 0.3	6.6 ± 1.3	-5.2 ± 3.1	12.3 ± 2.0	43.5 ± 9.3	(7)
Normal	27	17	247 ± 11	12.7 ± 0.9	5.4 ± 0.2	7.5 ± 0.8	-4.0 ± 1.3	11.9 ± 0.4	38.6 ± 4.3	(17)
Dyspedic	9	14	$33.9 \pm 9.3^{*†}$	$19.7 \pm 1.1^{*†}$	$6.9 \pm 0.3^{*†}$	$4.5 \pm 0.4^*$	$-14.0 \pm 1.5^{*†}$	11.6 ± 0.6	$8.5 \pm 1.7^{*†}$	(9)
RyR-1 expressing	6	7	$181 \pm 11^*$	13.5 ± 0.8	4.8 ± 0.2	4.8 ± 0.7	0.0 ± 2.8	11.2 ± 0.5	41.9 ± 11	(6)

I-V and Q-V data are from the number of myotubes indicated (*n*). Average values (\pm SEM) were obtained by fitting each myotube within a group separately to the appropriate equation (I-V, Eq. 1; Q-V, Eq. 4). The numbers of experiments used to calculate G_{max}/Q_{max} are indicated in parenthesis. The genotype of each culture used was determined by PCR analysis as described in methods. RyR1-expressing dyspedic myotubes were subject to patch-clamp experiments 2–4 d after cDNA microinjection. Q_{dys} (see Adams et al., 1990) was not subtracted from Q_{max} in calculations of G_{max}/Q_{max} as done previously (Nakai et al., 1996), since I_{dys} does not appear to be present in normal or dyspedic myotubes (see discussion).

*Compared with normal ($P < 0.001$), †compared with RyR-1 expressing ($P < 0.001$).

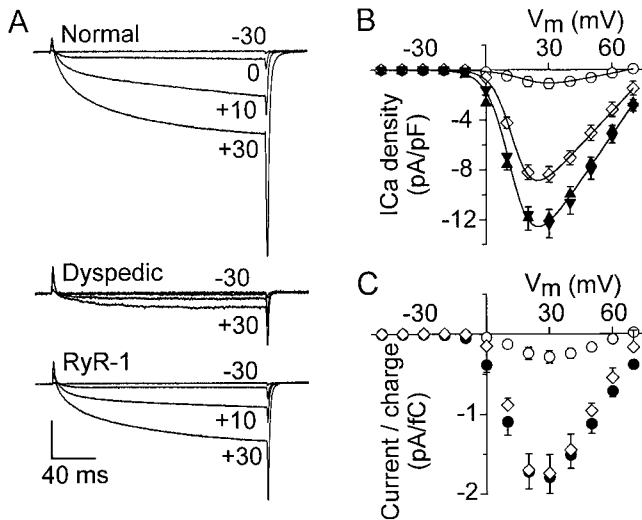


Figure 2. Voltage dependence of L-currents. (A) Family of calcium currents recorded from normal (top), dyspedic (middle), and RyR-1-expressing (bottom) dyspedic myotubes. The currents were elicited by 200-ms depolarizations from -50 mV to the indicated potential (mV) following a prepulse protocol (see methods) used to inactivate T-type Ca^{2+} currents. Vertical calibration corresponds to 6 pA/pF for the normal and RyR1-expressing myotubes and 2 pA/pF for the dyspedic myotube. (B) Average peak current density plotted as a function of membrane potential (V_m). Data were obtained from 13 RyR1 homozygous (+/+), 14 RyR1 heterozygous (+/-), 9 dyspedic (O), and 6 RyR1-expressing dyspedic (◇) myotubes. The average values (\pm SEM) for the parameters obtained by fitting each myotube within a group separately to Eq. 1 are given in Table I. The smooth solid lines through the data were generated by using Eq. 1 and the average values (I-V) given in Table I. Data for homozygous (+/+) and heterozygous (+/-) normal myotubes were each well represented by a single solid line obtained from the combined data (13 +/+ and 14 +/- myotubes). (C) Normal and RyR1-expressing dyspedic myotubes exhibit similar average current-to-charge ratios. Current-to-charge ratios were calculated by dividing the peak calcium current at each membrane potential by the maximum immobilization-resistant charge movement (Q_{max}) that was determined for each myotube. Data were obtained from 17 normal (●, 10 +/+ and 7 +/-), 9 dyspedic (O), and 6 RyR1-expressing dyspedic (◇) myotubes.

and RyR1-expressing dyspedic myotubes. The approximately fivefold difference in the current-to-charge (Fig. 2 C) and conductance-to-charge ($G_{\text{max}}/Q_{\text{max}}$) ratios between dyspedic myotubes and both normal and RyR1-expressing dyspedic myotubes (Table I) supports the conclusion that RyR1 increases L-channel open probability and/or unitary conductance (Nakai et al., 1996).

RyR1 Alters Two Kinetic Components of L-Current Activation

The slow activation time course of skeletal L-current in cultured mouse myotubes has often been approximated by fitting the data to a single exponential function (Tanabe et al., 1990; Dirksen and Beam, 1995; Strube et al., 1996; Beurg et al., 1997). However, L-current activation is apparently more complex. An adequate ($\chi^2 <$

0.005) quantitative description of activation in BC3H1 cells requires two exponential components (Caffrey, 1994). Fig. 3 A demonstrates that activation of L-currents in cultured skeletal myotubes also involves two kinetically distinct components. Single exponential fitting of normal L-currents failed to adequately describe current activation, particularly early during the depolarization (Fig. 3 A, left). However, fitting the data with the sum of two exponentials greatly improved (indicated by a >16 -fold reduction in the value of χ^2) the description of L-current activation (Fig. 3 A, right). The biexponential nature of the activation of the calcium current is best appreciated by replotting the normalized currents on a semilogarithmic scale (Fig. 3 A, bottom). The use of three exponential components did not significantly improve the fit of the data. The activation time course of the residual calcium current recorded from dyspedic myotubes was also best described by the sum of two exponential components (data not shown).

The second order exponential fitting procedure resulted in the extraction of the steady state amplitudes (A_{fast} and A_{slow}) and corresponding activation time constants (τ_{fast} and τ_{slow}) that comprise the macroscopic L-current. The influence of RyR1 on the amplitudes and time constants of macroscopic L-currents at $+40$ mV is summarized in Fig. 3, B–D. Amplitudes and time constants were compared between normal (N), dyspedic (Y), and RyR1-expressing (R) dyspedic myotubes after 200-ms depolarizations to $+40$ mV, a potential at which L-current conductance is maximal (Adams et al., 1990; Garcia et al., 1994; Dirksen and Beam, 1995). This analysis revealed that the marked reduction in dyspedic L-current arises from a parallel decrease in both A_{fast} (-2.20 ± 0.37 and -0.36 ± 0.03 for normal and dyspedic myotubes, respectively) and A_{slow} (-10.02 ± 1.04 and -1.14 ± 0.11 for normal and dyspedic myotubes, respectively). Thus, the fractional contribution of each component to the macroscopic L-current was similar in the presence and absence of RyR1 (Fig. 3 C). Interestingly, the faster overall activation of dyspedic L-currents (Nakai et al., 1996) arises from an approximately twofold reduction in both τ_{fast} and τ_{slow} (Fig. 3 D). Nuclear injection of dyspedic myotubes with wild-type RyR1 cDNA resulted in a marked increase in both A_{fast} and A_{slow} and also a corresponding increase in τ_{fast} and τ_{slow} (Fig. 3, B–D). Thus, the parallel dependence of both the amplitudes and time constants of the macroscopic L-current on the presence of RyR1 indicates that skeletal L-channels in cultured myotubes exhibit two distinct kinetic gating modes, each of which are modified by interaction with RyR1.

Bay K 8644 Accelerates Dyspedic L-Current Activation through a Preferential Increase in A_{fast}

The data illustrated in Table I and Fig. 3 suggest that RyR1 influences the functional conformation of the

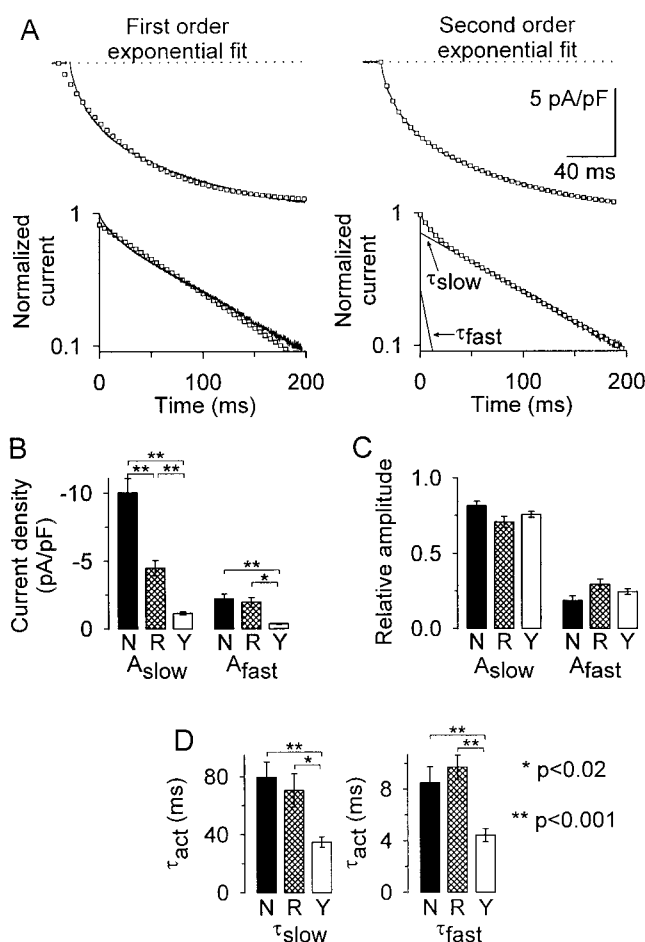


Figure 3. L-currents are best described by the sum of two exponential equations. (A) A representative calcium current (top) is illustrated for a normal myotube after 200-ms depolarizations to +40 mV. L-current activation was fitted according to either first (left) or second (right) order exponential functions (\square), as described in methods. The amplitudes and time constants obtained from the single-order exponential fitting was 9.26 pA/pF and 61.4 ms. Second-order exponential fitting resulted in the following values: $A_{slow} = 8.10$ pA/pF, $\tau_{slow} = 96.2$ ms, $A_{fast} = 2.97$ pA/pF, and $\tau_{fast} = 10.4$ ms. (Bottom) Semilogarithmic plots of the calcium current trace normalized to the peak current superimposed with the results of either a first (left) or second (right) order exponential fit (\square). The semilogarithmic plots demonstrate that an adequate description of current activation clearly requires two distinct exponential components (with time constants, τ_{fast} and τ_{slow}). (B–D) Average parameters obtained from second-order exponential fitting of L-currents obtained at +40 mV. Bars represent the average values from a total of six normal (N), seven dyspedic (Y), and eight RyR1-expressing dyspedic (R) myotubes. Data are shown for (B) current density, (C) relative amplitude (shown as $A_x/[A_{fast} + A_{slow}]$, where “ A_x ” represents the absolute steady state amplitude of either the fast or slow components), and (D) the time constants associated with the fast (τ_{fast}) and slow (τ_{slow}) components of the total current.

skeletal L-channel. Since DHP modulation of the activity and voltage dependence L-channels is state dependent (Hille, 1992), we set out to evaluate the effects of RyR1 on the DHP modulation of L-channels in cul-

tured skeletal myotubes. We first compared whole-cell calcium currents in the absence (control) and presence of the pure DHP agonist, (–) Bay K 8644 (5 μ M). Fig. 4 A shows representative L-currents recorded from normal (left) and dyspedic (right) myotubes elicited by 200-ms depolarizations to +40 mV. To emphasize kinetic differences, control traces are shown after normalization to the peak current recorded in the presence of (–) Bay K 8644 (5 μ M). In both myotubes, 5 μ M (–) Bay K 8644 produced a 46% increase in peak calcium current (see also Fig. 5, A and C) and a significant acceleration in the activation time course.

As demonstrated in Fig. 3 A, L-current activation was clearly best described by the sum of two exponential functions, and this becomes even more evident in the presence of DHP (where the second-order fit reduced $\chi^2 > 43$ -fold, Fig. 4 A, left). This analysis revealed that at +40 mV the DHP-induced acceleration in L-channel activation kinetics in normal myotubes arises primarily from a preferential increase in the amplitude of the fast component (A_{fast}) of L-current (Fig. 4 B, left). Specifically, (–) Bay K 8644 caused a significant increase ($83 \pm 12\%$, $n = 6$) in the magnitude of A_{fast} , without significantly altering A_{slow} . However, the time constants of each component (τ_{fast} and τ_{slow}) were not significantly altered in the presence of the DHP agonist (Fig. 4 B, right). In dyspedic myotubes at +40 mV, (–) Bay K 8644 induced an increase in A_{fast} ($174 \pm 30\%$, $n = 7$) without significantly altering the magnitudes of A_{slow} , τ_{fast} , or τ_{slow} (Fig. 4 C). Consequently, in dyspedic myotubes, the DHP agonist increased the relative contribution of A_{fast} to the total L-current (at +40 mV, $A_{fast}/[A_{fast} + A_{slow}]$ was 0.24 ± 0.02 in control and 0.49 ± 0.02 in 5 μ M (–) Bay K 8644, $P < 0.001$). Thus, at +40 mV, (–) Bay K 8644 preferentially augmented the magnitude of A_{fast} in both normal and dyspedic myotubes without altering A_{slow} , τ_{fast} , or τ_{slow} .

The data described in Fig. 4 were obtained for test pulses to +40 mV, a potential at which L-channel conductance is maximal in both the presence and absence of DHP agonist. The effects of (–) Bay K 8644 (5 μ M) on the voltage dependence of macroscopic skeletal L-currents and its component parts (A_{fast} and A_{slow}) are summarized in Fig. 5. The peak I-V relationships of normal (Fig. 5 A) and dyspedic (C) myotubes were obtained in the absence (\bullet) and presence (\circ) of (–) Bay K 8644 (5 μ M). In both types of myotubes, the DHP agonist produced both a similar increase in total L-current density and a hyperpolarizing shift (~ 10 mV, Table II) in the macroscopic I-V relation. However, these effects on the overall macroscopic currents arise from qualitatively distinct alterations in the two kinetic components of skeletal L-current. In Fig. 5, the magnitudes of A_{fast} and A_{slow} in normal (B) and dyspedic (D) myotubes were normalized by the average peak control value for

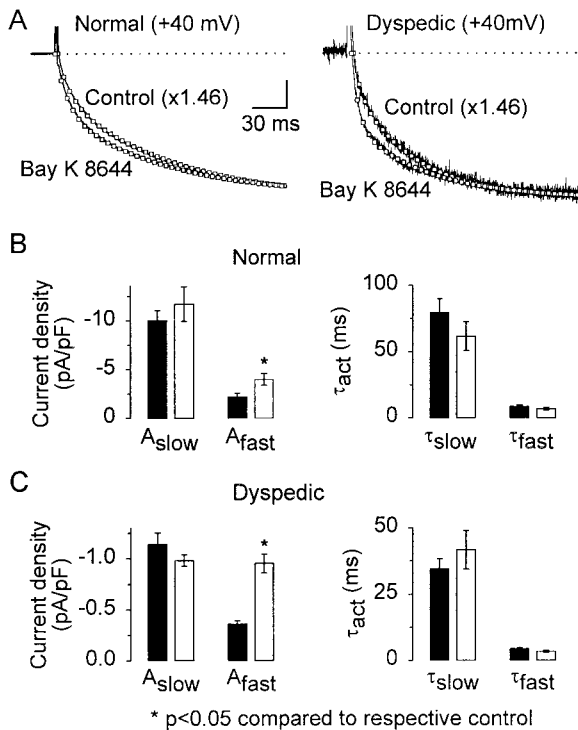


Figure 4. Effects of DHP agonist on the two components of macroscopic L-current. (A) Representative L-currents recorded from a normal (left) and a dyspedic (right) myotube in the absence (control) and presence of 5 μM (-) Bay K 8644. Current traces were fitted according to a second-order exponential function (\square , superimposed over raw data). Both control traces have been scaled (1.46 \times) to the peak of the L-current recorded in the presence of DHP. The vertical calibration corresponds to 3 and 0.3 pA/pF for the normal and dyspedic L-current traces recorded in the presence of DHP, respectively. (B) Average values obtained for current density (left) and τ_{act} (right) obtained from second-order exponential fitting of data obtained at +40 mV. Data were tabulated from the analysis of calcium currents that were recorded in the absence (black bars) and presence (white bars) of 5 μM (-) Bay K 8644. Values represent means \pm SEM of six experiments in normal myotubes and seven experiments in dyspedic myotubes. (-) Bay K 8644 selectively augmented the fast amplitude (A_{fast}) component in both normal (\sim 1.8-fold) and dyspedic (\sim 2.7-fold) myotubes, without significantly altering τ_{fast} or τ_{slow} . (C) Average values obtained for current density (left) and τ_{act} (right) obtained from second-order exponential fitting of data obtained at +40 mV. Data were tabulated from the analysis of calcium currents that were recorded in the absence (black bars) and presence (white bars) of 5 μM (-) Bay K 8644. Values represent means \pm SEM of six experiments in normal myotubes and seven experiments in dyspedic myotubes. (-) Bay K 8644 selectively augmented the fast amplitude (A_{fast}) component in both normal (\sim 1.8-fold) and dyspedic (\sim 2.7-fold) myotubes, without significantly altering τ_{fast} or τ_{slow} . * $p < 0.05$ compared to respective control.

each data set (A_{slow} and A_{fast} were: 11.89 ± 1.10 and 2.30 ± 0.40 pA/pF for normal myotubes, and 1.23 ± 0.16 and 0.47 ± 0.06 pA/pF for dyspedic myotubes). This analysis revealed that, even under control conditions, A_{fast} activates \sim 10 mV more hyperpolarized than A_{slow} . In normal myotubes, (-) Bay K 8644 increased (up to approximately twofold) the normalized magnitude of both A_{fast} and A_{slow} . In addition, the DHP-induced hyperpolarizing shift in the voltage dependence of L-channel activation is reflected as a selective shift in the voltage dependence of A_{slow} . Interestingly, (-) Bay K 8644 produced an approximately threefold increase in A_{fast} in

the absence of an alteration in the magnitude of A_{slow} in dyspedic myotubes. The remarkable DHP insensitivity of A_{slow} in dyspedic myotubes indicates that the RyR1 protein imparts a strong influence on the state-dependent action of DHP agonists on skeletal L-channels.

RyR1 Modifies Skeletal L-Channel Divalent Conductance

Equimolar substitution of Ba^{2+} for extracellular Ca^{2+} produces an increase in peak L-current and a hyperpolarizing shift in the voltage dependence of channel activation in cardiac muscle (Kass and Sanguinetti, 1984). Increased L-current amplitude has been attributed to a higher L-channel conductance to Ba^{2+} (Fox et al., 1987), while the shift in channel activation involves differences in the ability of Ba^{2+} and Ca^{2+} ions to screen external surface charges (Hille, 1992). A similar substitution produces a smaller increase in L-current density and a similar hyperpolarizing shift in channel activation in skeletal muscle (Tanabe et al., 1990). We investigated the influence of the RyR1 protein on the effects of equimolar substitution of Ba^{2+} for extracellular Ca^{2+} on skeletal L-currents in Fig. 6. In both normal and dyspedic myotubes, L-channel activation was shifted \sim 10 mV in the hyperpolarized direction upon replacement of extracellular Ca^{2+} with Ba^{2+} (Fig. 6; Table II). In normal myotubes, peak L-current magnitude (Fig. 6 B, a) and conductance (Table II) were increased ($P < 0.01$) nearly 40% with Ba^{2+} as the extracellular charge carrier. In contrast, peak L-current magnitude (Fig. 6 B, c) and conductance (Table II) were unaltered upon the identical divalent substitution in dyspedic myotubes.

The relative contribution of A_{fast} and A_{slow} to the macroscopic Ca^{2+} and Ba^{2+} currents (Fig. 6 B, b and d) were extracted by fitting a second-order exponential function to the activation phase of the ionic currents (Fig. 6 A). Substitution of Ba^{2+} for extracellular Ca^{2+} increased both A_{fast} and A_{slow} in normal myotubes (Fig. 6 B, b) without greatly altering either τ_{fast} or τ_{slow} (data not shown). The identical divalent substitution failed to significantly alter the magnitude of either A_{fast} or A_{slow} in dyspedic myotubes (Fig. 6 B, d). Nevertheless, extracellular Ba^{2+} substitution caused a hyperpolarizing shift in the voltage dependence of both A_{fast} and A_{slow} in normal and dyspedic myotubes. Thus, the skeletal muscle ryanodine receptor appears to influence relative L-channel divalent conductance, but not the differential ability of Ca^{2+} and Ba^{2+} ions to modify external surface charge. These data suggest that the interaction of RyR1 with the skeletal muscle DHPR may exert long-range effects on the functional conformation of the pore of the skeletal L-channel. However, a direct evaluation of the effects of RyR1 on skeletal L-channel selectivity must await a systematic determination of the monovalent and divalent permeability sequence of L-channels in normal and dyspedic myotubes.

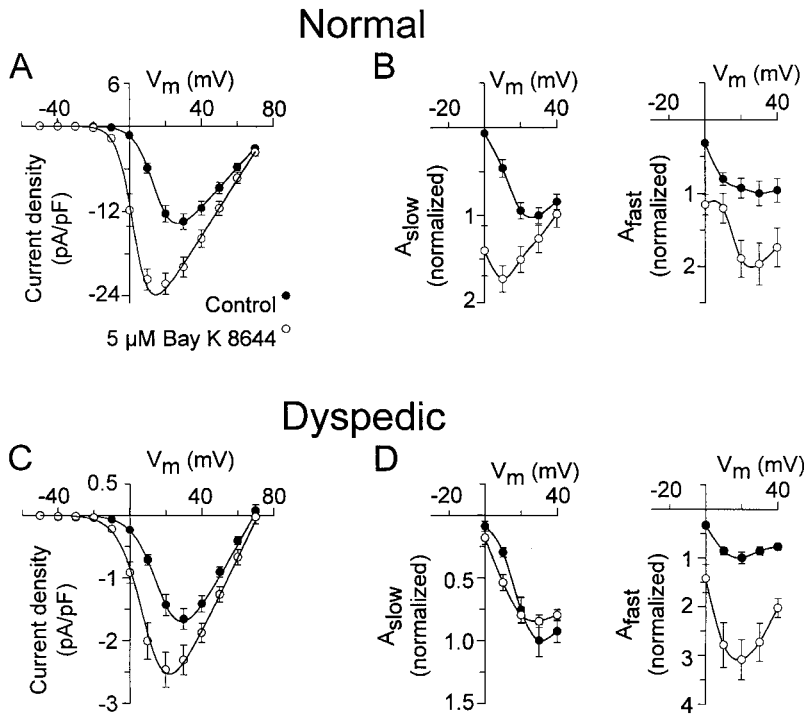


Figure 5. Voltage dependence of the stimulatory effects of DHP agonist on the fast and slow components of macroscopic L-current. Average L-current-voltage relationships obtained from six normal (A) and seven dyspedic (C) myotubes in the absence (●) and presence (○) of 5 μ M (–) Bay K 8644. (B and D) A_{fast} and A_{slow} were determined for current traces from 0 to +40 mV (see methods) and normalized to their maximal value obtained in the absence of DHP. Normalized A_{fast} and A_{slow} values were then plotted as a function of membrane potential (V_m). Absolute peak values for the two components of the calcium current in the absence of DHP were (pA/pF): $A_{slow} = 11.89 \pm 1.10$, $A_{fast} = 2.30 \pm 0.40$ for normal myotubes, and $A_{slow} = 1.23 \pm 0.16$, $A_{fast} = 0.47 \pm 0.06$ for dyspedic myotubes. Neither τ_{fast} nor τ_{slow} were significantly altered by 5 μ M (–) Bay K 8644 at any potential (data not shown).

DISCUSSION

In skeletal muscle, the coupling of sarcolemmal depolarization to the release of SR calcium is thought to involve a direct physical interaction between the DHPR and the RyR1. If the interaction of RyR1 with the DHPR stabilizes certain L-channel conformational states by altering transition rates between states, then disruption of this interaction may result in altered L-channel function. However, no study has systematically characterized the influence of RyR1 on the biophysical and pharmacological properties of the skeletal L-current. Consequently, we have evaluated the influence of RyR1 on the expression level, voltage dependence, activation rate, DHP modulation, and divalent conductance of the skeletal L-channel. Our results indicate that the density of functional sarcolemmal L-channels is reduced by $\sim 40\%$ in dyspedic myotubes compared

with that of myotubes derived from their phenotypically normal littermates. We also demonstrated that dyspedic L-currents exhibit accelerated activation (τ_{fast} and τ_{slow}), a greater separation between Q-V and G-V relationships ($[V_{G1/2} - V_{Q1/2}]$ was 16.7, 33.7, and 13.5 mV for normal, dyspedic, and RyR1-expressing dyspedic myotubes, respectively), and similar macroscopic conductances to Ca^{2+} and Ba^{2+} . The ability of RyR1 to enhance the coupling between charge movement and pore opening (i.e., reduce Q-V/G-V separation) and alter the relative conductance to divalent ions (Ca^{2+} versus Ba^{2+}) suggests that RyR1 imparts long-range effects on the conformational state of the pore of the skeletal L-channel. In addition, (–) Bay K 8644 increased the magnitude of both the fast (A_{fast}) and slow (A_{slow}) components of the total L-current in normal myotubes, but only enhanced the fast component in dyspedic myotubes. Thus, our results indicate that the presence of

TABLE II
Parameters of Fitted I-V Curves

	Normal myotubes			Dyspedic myotubes				
	<i>n</i>	G_{max} nS/nF	$V_{G1/2}$ mV	k_G mV	<i>n</i>	G_{max} nS/nF	$V_{G1/2}$ mV	k_G mV
Control	6	283 \pm 22	14.9 \pm 0.7	5.4 \pm 0.2	7	51.1 \pm 5.4	18.0 \pm 0.6	6.9 \pm 0.6
(–) Bay K 8644	6	398 \pm 25*	2.91 \pm 1.6*	4.5 \pm 0.4	7	59.9 \pm 5.1	9.61 \pm 1.2*	6.9 \pm 0.4
10 Ca^{2+}	11	254 \pm 9.2	12.5 \pm 1.3	4.8 \pm 0.2	8	42.7 \pm 2.7	15.0 \pm 1.2	6.9 \pm 0.2
10 Ba^{2+}	11	348 \pm 24 [†]	2.39 \pm 1.3 [†]	3.7 \pm 0.2 [†]	8	50.0 \pm 2.9	6.87 \pm 1.1 [†]	5.6 \pm 0.3 [†]

Values (mean \pm SEM) were obtained as described in Table I. Data are from the number of myotubes indicated (*n*).

*Compared with control ($P < 0.01$), [†]compared with 10 Ca^{2+} ($P < 0.01$).

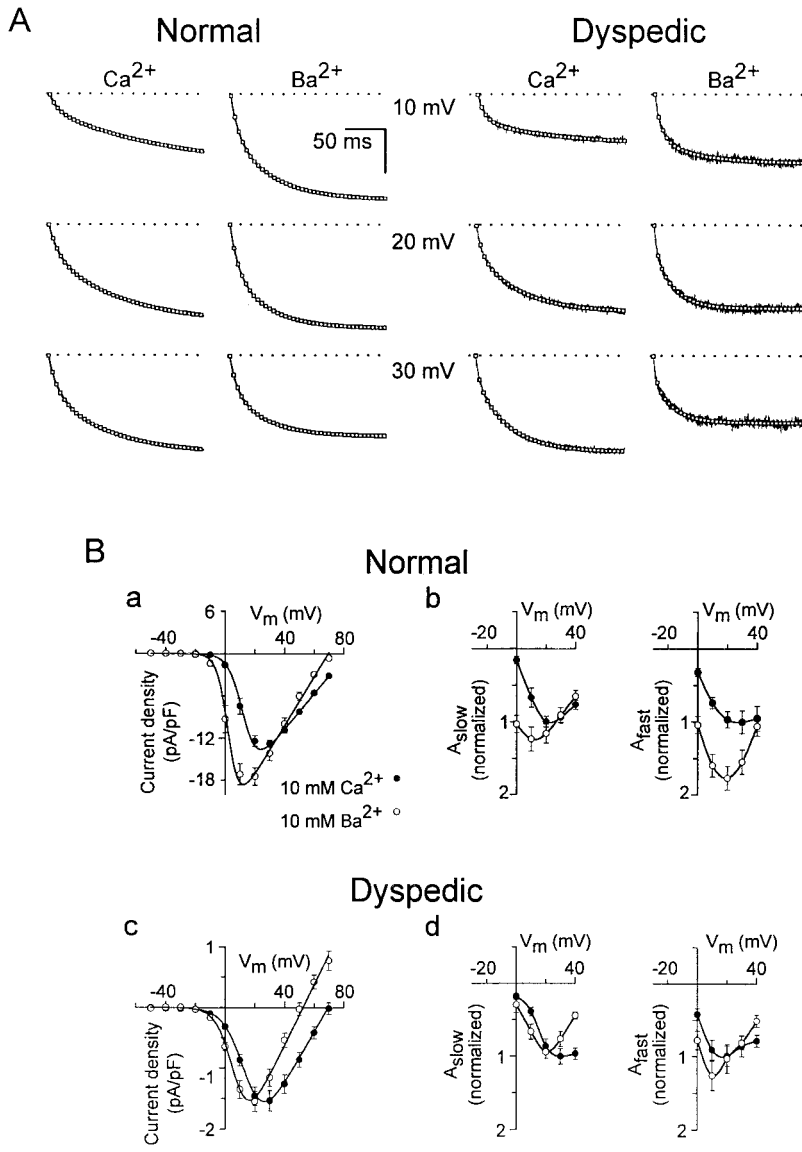


Figure 6. Voltage dependence of the effects of divalent charge carrier on the fast and slow components of macroscopic L-current. (A) Representative L-currents recorded from a normal (left) and dyspedic (right) myotube obtained in the presence of either 10 mM extracellular Ca²⁺ (Ca²⁺) or 10 mM extracellular Ba²⁺ (Ba²⁺). Current traces were fitted according to a second-order exponential function (□, superimposed over raw data). The vertical calibration corresponds to 2.5 and 0.5 nA for the normal and dyspedic myotubes, respectively. (B) L-current-voltage relationships from 11 normal (a) and seven dyspedic (c) myotubes recorded as in A. A_{slow} and A_{fast} values (b and d) were obtained and normalized as described in Fig. 5. Absolute peak values for the two components of the calcium current were (pA/pF): A_{slow} = 10.89 ± 0.80, A_{fast} = 2.28 ± 0.36 for normal myotubes, and A_{slow} = 1.12 ± 0.12, A_{fast} = 0.47 ± 0.07 for dyspedic myotubes.

RyR1 in skeletal muscle imparts a strong influence on several essential properties of the skeletal L-channel.

RyR1 Promotes L-Channel Expression

Previous studies have demonstrated that dyspedic muscle exhibits a 25–50% reduction in total DHP binding capacity compared with normal muscle (Fleig et al., 1996; Buck et al., 1997). Our finding that Q_{max} of dyspedic myotubes is reduced ~40% compared with normal myotubes is in agreement with these reports and indicates that RyR1 promotes DHP expression in skeletal muscle. However, this 40% reduction in DHP expression cannot fully account for the ~90% reduction in the value of G_{max} in dyspedic myotubes. Even after normalization of peak currents (Fig. 2) and G_{max} (Table I) by Q_{max}, DHPs in normal myotubes possess an approximately fivefold higher Ca²⁺-conducting activity compared with that of dyspedic myotubes. Thus, our results

support the conclusion of Nakai et al. (1996) that RyR1 enhances either the open probability and/or the unitary conductance of skeletal L-channels. Interestingly, DHPR Ca²⁺-conducting activity (I_{Ca}/Q_{max} and G_{max}/Q_{max}) was completely restored 2–4 d after nuclear injection of dyspedic myotubes with RyR1 cDNA without altering the magnitude of Q_{max}. Apparently, introduction of RyR1 proteins into dyspedic myotubes restores existing L-channel activity before increasing DHPR expression (as reflected in Q_{max}). It will be important for future experiments to determine whether or not long-term expression of RyR1 is able to restore Q_{max} to a value similar to that of normal myotubes and whether these changes are also associated with alterations in EC coupling. Interestingly, the preferential influx of Ca²⁺ through L-channels activates the calcium/calmodulin/NF-ATc transcription pathway and results in the induction of the type 1 1,4,5-inositol trisphosphate receptor in

hippocampal neurons (Graef et al., 1999). Thus, it will be important to determine whether the enhancement of L-channel expression in skeletal myotubes also involves activation of a calcium-mediated transcription pathway (via Ca^{2+} influx and/or SR Ca^{2+} release).

Two Kinetic Components of L-Current Activation

The activation kinetics of skeletal L-currents in cultured myotubes has often been approximated by fitting the activation time course to a single exponential function. This approach has provided a convenient means for making qualitative comparisons in channel kinetics under different conditions (Tanabe et al., 1991; Dirksen and Beam, 1995; Beurg et al., 1997). However, a precise quantitative description of skeletal L-current activation appears to require the sum of two exponential components (Fig. 3; and see Caffrey, 1994). For example, Caffrey (1994) demonstrated that macroscopic L-current activation in BC3H1 myotubes was best described by the sum of two ascending exponential terms with time constants ($\tau_1 = 2\text{--}20$ ms and $\tau_2 = 10\text{--}200$ ms) similar to those reported here. Moreover, the voltage dependence and relative contribution of the faster component in BC3H1 cells ($\sim 25\%$ at $+40$ mV) is comparable with our results using primary myotube cultures. Our analyses indicate that while a single exponential often results in a reasonable approximation of L-channel activation at strong depolarizations (>20 mV), two activation terms are clearly required under conditions that enhance the relative contribution of the fast component of L-current activation. An increase in the relative contribution of A_{fast} results in a clear bi-exponential activation for L-currents activated at threshold potentials (e.g., -10 mV) and for L-currents in dyspedic myotubes treated with (–) Bay K 8644 (Fig. 4 A). In addition, we have recently reported that prolonged depolarization markedly increases the relative contribution of A_{fast} to the total L-current, resulting in a clearly bi-exponential L-channel activation time course (O'Connell and Dirksen, 2000).

Apparent channel activation can be altered when a significant degree of inactivation occurs during the activation process. Thus, inactivation occurring during our 200-ms test pulses could influence the kinetic properties of L-channel activation (A_{fast} , τ_{fast} , A_{slow} and τ_{slow}) reported here. Since we have not systematically characterized inactivation in normal and dyspedic myotubes in this study, we cannot rule out a possible contribution of inactivation to the effects of RyR1 on the kinetic properties of L-channel activation. However, any effects of inactivation on apparent L-channel activation would be anticipated to be minimal in our experiments since inactivation of L-currents is very slow ($\sim 25\times$ slower than τ_{slow} described here) in myotubes (Harasztosi et al., 1999).

Normal myotubes possess T-type Ca^{2+} channels (Adams et al., 1990; Dirksen and Beam, 1995) that exhibit a similar rate of activation as that associated with A_{fast} . However, our data strongly suggest that A_{fast} does not arise from T-type channels. First of all, the sum of two exponentials is also required to fit L-current activation observed in normal myotubes that exhibit vanishingly small (or undetectable) T-type Ca^{2+} current (data not shown). Moreover, the magnitude of A_{fast} peaks at approximately $+30$ mV, ~ 40 mV more depolarized than the peak of the current–voltage relationship of T-type Ca^{2+} channels (Garcia and Beam, 1994). In addition, A_{fast} is potentiated by (–) Bay K 8644 (Figs. 4 and 5) and exhibits a greater conductance for Ba^{2+} than Ca^{2+} (Fig. 6 B). These observations clearly contrast with the classic profile of T-type Ca^{2+} channels (Hille, 1992), and are most consistent with the notion that A_{fast} originates from L-type Ca^{2+} channels.

Dysgenic myotubes, which lack an intact gene for the skeletal muscle DHP, exhibit a rapidly activating, DHP-sensitive L-current (I_{dys} ; Adams and Beam, 1989) that may be attributable to the cardiac α_{1C} subunit. It is also likely that the channels that account for I_{dys} make a significant contribution to the residual immobilization-resistant intramembrane charge movement found in dysgenic myotubes (Q_{dys} ; Adams et al., 1990). The fast component of L-current activation (A_{fast}) described in this study resembles I_{dys} in that both currents peak at approximately $+20$ mV, activate rapidly ($\tau_{\text{act}} \sim 5$ ms), and are augmented two- to threefold by (–) Bay K 8644. However, several findings suggest that the fast component of skeletal L-current activation is distinct from I_{dys} . For example, I_{dys} is more strongly stimulated by (–) Bay K 8644 than L-current in normal myotubes (Adams and Beam, 1989; Strube et al., 1998). However, the data in Fig. 5 shows that (–) Bay K 8644 stimulates both kinetic components of L-current activation (A_{fast} and A_{slow}) to a roughly similar degree. In addition, expression of RyR1 in dyspedic myotubes causes a marked increase in A_{fast} without altering the magnitude of Q_{max} (Fig. 3), an observation clearly inconsistent with I_{dys} as the identity of A_{fast} . Finally, substitution of Ba^{2+} for extracellular Ca^{2+} doubles the size of I_{dys} , but only enhanced A_{fast} in normal, and not dyspedic, myotubes (Fig. 6, B and D). Thus, our data are inconsistent with I_{dys} as the identity of the fast component of skeletal L-channel activation, but rather support the notion that A_{fast} represents an intrinsic gating property of the skeletal L-channel.

It is uncertain whether the two components of L-channel activation in mouse skeletal myotubes reflect the gating of separate ion channels or two gating modes of a single Ca^{2+} channel protein. However, our data support the latter possibility since RyR1 regulates several properties of these two components in a quanti-

tatively similar manner. For example, A_{fast} and A_{slow} are each reduced approximately sevenfold in the absence of RyR1, resulting in a constant relative contribution of fast and slow components to the total L-current in both normal and dyspedic myotubes. Interestingly, RyR1 expression increased A_{fast} to a value comparable with that of normal myotubes and only partially restored A_{slow} , resulting in a moderately significant ($P < 0.05$) increase in the relative contribution of A_{fast} . In addition, both τ_{fast} and τ_{slow} are approximately twofold faster in dyspedic myotubes, and expression of RyR1 in dyspedic myotubes restores both τ_{fast} and τ_{slow} to values similar to those of normal myotubes. Based on single channel recordings (Dirksen and Beam, 1996) and gating current measurements (Dirksen and Beam, 1999), slow skeletal L-channel activation has been accounted for by a linear reaction scheme in which the rate-limiting transition exhibits an asymmetric voltage dependence. According to this scheme, faster L-channel activation observed in the absence of RyR1 (dyspedic myotubes) could arise from an increase in the forward rate constant (“ δ ” in the model of Dirksen and Beam, 1996) governing this rate-limiting transition. In this way, RyR1 may act like a tether stabilizing one or more of the closed states traversed during channel activation. According to this hypothesis, single L-channels recorded from dyspedic myotubes would be anticipated to exhibit a briefer time to first opening after depolarization and possibly a decrease in channel closed times.

Distribution and Targeting of L-Channels in Dyspedic and RyR1-expressing Dyspedic Myotubes

Skeletal muscle dihydropyridine receptors and ryanodine receptors colocalize in clusters that are randomly distributed in punctate foci throughout the muscle cell (Flucher et al., 1993; Franzini-Armstrong and Jorgensen, 1994). These clusters occur at junctions between terminal SR and both the surface and transverse tubule (t-tubules) membranes and presumably represent functional sites of skeletal muscle EC coupling (Franzini-Armstrong et al., 1991; Franzini-Armstrong and Jorgensen, 1994). Within these junctions, SR Ca^{2+} release channels are packed in highly ordered arrays. Moreover, clusters of four evenly spaced membrane particles (tetrads), apparently representing DHPRs, are positioned in the sarcolemma such that each particle is located immediately above each of the four RyR1 subunits of the release channel homotetramer (Block et al., 1988). In dyspedic myotubes, junctions containing large clusters of DHPRs are present periodically throughout the sarcolemma (though in a limited number; Takekura et al., 1995). Thus, RyR1 proteins are not required for the targeting of DHPRs to the junctional domains. However, the junctional clusters of DHPRs in dyspedic myo-

tubes are not organized into tetrads, indicating that RyR1 proteins dictate the positioning of DHPRs into tetrads (Takekura and Franzini-Armstrong, 1999).

Our results, in which injection with RyR1 cDNA restores both the I_{Ca}/Q_{max} (Fig. 2) and G_{max}/Q_{max} (Table I) ratios of dyspedic myotubes to values comparable with those of normal myotubes, indicate that the vast majority of dyspedic sarcolemmal L-channels are functionally “recoupled” upon RyR1 expression. Thus, it is possible that the expressed RyR1 proteins are efficiently targeted to the majority of junctions throughout the injected dyspedic myotubes. However, Lorenzon et al. (1999) demonstrated that the distribution of GFP-tagged RyR1 proteins expressed in dyspedic myotubes are restricted to the region surrounding the site of injection. Since our experiments were performed on morphologically compact myotubes and we have not monitored RyR1 localization after nuclear injection, the spatial restrictions of the expressed RyR1 proteins in our experiments cannot be easily inferred. However, it will be interesting to determine whether the periodic distribution of DHPRs throughout the dyspedic sarcolemma are reorganized in such a way as to permit interaction with a restricted distribution of RyR1 proteins.

RyR1 Acts as an Allosteric Modulator of Skeletal L-Channel Activity

The functional properties of voltage-dependent Ca^{2+} channels are markedly influenced by direct interactions with auxiliary Ca^{2+} channel subunits and intracellular signaling proteins. With regard to L-channels, β -subunits augment peak Ca^{2+} current by increasing the number of channels in the surface membrane (Lacerda et al., 1991; Singer et al., 1991; Wei, et al., 1991), increasing channel open probability (Neely et al., 1993; Shistik et al., 1995), and facilitating channel pore opening (Neely et al., 1993). In addition, β -subunits also accelerate the kinetics of L-channel activation and inactivation (Singer et al., 1991; Wei et al., 1991) and shift activation to more hyperpolarized voltages (Neely et al., 1993). In skeletal muscle, the β_1 -subunit accelerates L-channel activation (Lacerda et al., 1991; Varadi et al., 1991), augments total DHP binding (Lacerda et al., 1991), and promotes the targeting of α_1 -subunits to the plasma membrane (Strube et al., 1996; Beurg et al., 1997). In addition, the β_{1a} -subunit, and not the β_{2a} -subunit, restores both L-current and EC coupling in myotubes derived from mice carrying a null mutation in the β_1 gene (Beurg et al., 1999). The $\alpha_2\text{-}\delta$ -subunit generally acts to potentiate the effects of β subunits on L-current amplitude and kinetics (Singer et al., 1991) and both the $\alpha_2\text{-}\delta$ - and β -subunits enhance DHP binding to L-channels (Singer et al., 1991).

Several important intracellular signaling molecules

are also known to interact and modify the functional properties of voltage-dependent Ca^{2+} channels. For example, the properties of neuronal N- and P/Q-type Ca^{2+} channels are modulated by interaction with synaptic membrane proteins (e.g., syntaxin and the 25-kD synaptosome-associated protein, SNAP25) that control vesicle docking and membrane fusion during neurotransmitter release (for review, see Catterall, 1999). G protein β/γ -subunits directly inhibit neuronal N-, P/Q-, and R-type Ca^{2+} channels by reducing current amplitude, slowing channel activation, and shifting channel activation to more depolarized potentials (for review, see Dolphin, 1998). Additionally, Ca^{2+} -dependent inactivation of cardiac L-channels has recently been suggested to involve a constitutive interaction between calmodulin and the Ca^{2+} -channel complex (Peterson et al., 1999). The interaction of ryanodine receptors with L-channels in skeletal muscle (Nakai et al., 1996) and neurons (Chavis et al., 1996) causes an enhancement of Ca^{2+} flux through these channels. Our results demonstrate that the skeletal muscle ryanodine receptor also modifies other important channel properties, including L-channel expression level, voltage dependence and kinetics of activation, modulation by DHPs, and the relative conductance to Ca^{2+} and Ba^{2+} . These results support the notion that RyR1 is an important allosteric modulator of the skeletal L-channel, analogous to that of a conventional Ca^{2+} channel accessory subunit.

We thank Drs. Kurt G. Beam and Paul D. Allen for providing us access to the dyspedic mice used in this study, as well as for their advice and continued support. We also thank Dr. Ted Begenisich for helpful discussions and comments on the manuscript and Linda Groom for excellent technical assistance.

This work was supported by National Institutes of Health grant AR44657 (R.T. Dirksen), a Neuromuscular Disease Research grant (R.T. Dirksen), and CONACYT postdoctoral fellowship 990236 (G. Avila).

Submitted: 7 December 1999

Revised: 22 February 2000

Accepted: 23 February 2000

REFERENCES

- Adams, B.A., and K.G. Beam. 1989. A novel calcium current in dysgenic skeletal muscle. *J. Gen. Physiol.* 94:429-444.
- Adams, B.A., T. Tanabe, A. Mikami, S. Numa, and K.G. Beam. 1990. Intramembrane charge movement restored in dysgenic skeletal muscle by injection of dihydropyridine receptor cDNAs. *Nature* 346:569-572.
- Armstrong, C.M., F.M. Bezanilla, and P. Horowicz. 1972. Twitches in the presence of ethylene glycol bis-(aminoethyl ether)-*N,N'*-tetraacetic acid. *Biochim. Biophys. Acta* 267:605-608.
- Beurg, M., M. Sukhareva, C.A. Ahren, M.W. Conklin, E. Perez-Reyes, P.A. Powers, R.G. Gregg, and R. Coronado. 1999. Differential regulation of skeletal muscle L-type Ca^{2+} current and excitation-contraction coupling by the dihydropyridine receptor β_1 subunit. *Biophys. J.* 76:1744-1756.
- Beurg, M., M. Sukhareva, C. Strube, P.A. Powers, R.G. Gregg, and R. Coronado. 1997. Recovery of Ca^{2+} current, charge movements, and Ca^{2+} transients in myotubes deficient in dihydropyridine receptor β_1 subunit transfected with β_1 cDNA. *Biophys. J.* 73:807-818.
- Block, B.A., T. Imagawa, K.P. Campbell, and C. Franzini-Armstrong. 1988. Structural evidence for direct interaction between the molecular components of the transverse tubule/sarcoplasmic reticulum junction in skeletal muscle. *J. Cell Biol.* 107:2587-2600.
- Buck, E.D., H.T. Nguyen, I.N. Pessah, and P.D. Allen. 1997. Dyspedic mouse skeletal muscle expresses major elements of the triadic junction, but lacks detectable ryanodine receptor protein and function. *J. Biol. Chem.* 272:7360-7367.
- Caffrey, J.M. 1994. Kinetic properties of skeletal-muscle-like high-threshold calcium currents in a non-fusing muscle cell line. *Pflügers Arch.* 427:277-288.
- Catterall, W.A. 1999. Interactions of presynaptic Ca^{2+} channels and SNARE proteins in neurotransmitter release. *Ann. NY Acad. Sci.* 868:144-159.
- Chavis, P., L. Fagni, J.B. Lansman, and J. Bockaert. 1996. Functional coupling between ryanodine receptors and L-type calcium channels in neurons. *Nature* 382:719-722.
- Dirksen, R.T., and K.G. Beam. 1995. Single calcium channel behavior in native skeletal muscle. *J. Gen. Physiol.* 105:227-247.
- Dirksen, R.T., and K.G. Beam. 1996. Unitary behavior of skeletal, cardiac, and chimeric L-type Ca^{2+} channels expressed in dysgenic myotubes. *J. Gen. Physiol.* 107:731-742.
- Dirksen, R.T., and K.G. Beam. 1999. Role of calcium permeation in dihydropyridine receptor function: insights into channel gating and excitation-contraction coupling. *J. Gen. Physiol.* 114:393-404.
- Dolphin, A.C. 1998. Mechanisms of modulation of voltage-dependent calcium channels by G-proteins. *J. Physiol.* 506:3-11.
- Fleig, A., H. Takeshima, and R. Penner. 1996. Absence of Ca^{2+} current facilitation in skeletal muscle of transgenic mice lacking the type 1 ryanodine receptor. *J. Physiol.* 496:339-345.
- Flucher, B.E., S.B. Andrews, S. Fleischer, A.R. Marks, A. Caswell, and J.A. Powell. 1993. Triad formation: organization and function of the sarcoplasmic reticulum calcium release channel and triadin in normal and dysgenic muscle in vitro. *J. Cell. Biol.* 123:1161-1174.
- Fox, A.P., M.C. Nowycky, and R.W. Tsien. 1987. Kinetic and pharmacological properties distinguishing three types of calcium currents in chick sensory neurones. *J. Physiol.* 394:149-172.
- Franzini-Armstrong, C., and A.O. Jorgensen. 1994. Structure and development of E-C coupling units in skeletal muscle. *Annu. Rev. Physiol.* 56:509-534.
- Franzini-Armstrong, C., M. Pincon-Raymond, and F. Rieger. 1991. Muscle fibers from dysgenic mouse in vivo lack a surface component of peripheral couplings. *Dev. Biol.* 146:364-376.
- Garcia, J., and K.G. Beam. 1994. Measurement of calcium transients and slow calcium current in myotubes. *J. Gen. Physiol.* 103:107-123.
- Garcia, J., T. Tanabe, and K.G. Beam. 1994. Relationship of calcium transients to calcium currents and charge movements in myotubes expressing skeletal and cardiac dihydropyridine receptors. *J. Gen. Physiol.* 103:125-147.
- Grabner, M., R.T. Dirksen, N. Suda, and K.G. Beam. 1999. The II-III loop of the skeletal muscle dihydropyridine receptor is responsible for the bi-directional coupling with the ryanodine receptor. *J. Biol. Chem.* 274:21913-21919.
- Graef, I.A., P.G. Mermelstein, K. Stankunas, J.R. Neilson, K. Deisseroth, R.W. Tsien, and G.R. Crabtree. 1999. L-type calcium channels and GSK-3 regulate the activity of NF- $\text{Atc}4$ in hippocampal neurons. *Nature* 401:703-708.
- Hamill, O.P., A. Marty, E. Neher, B. Sakmann, and F.J. Sigworth. 1981. Improved patch-clamp techniques for high-resolution cur-

- rent recording from cells and cell-free membrane patches. *Pflügers Arch.* 391:85–100.
- Harasztosi, C., I. Sipos, L. Kovacs, and W. Melzer. 1999. Kinetics of inactivation and restoration of the L-type calcium current in human myotubes. *J. Physiol.* 516:129–138.
- Hille, B. 1992. *Ionic Channels of Excitable Membranes*. 2nd ed. Sinauer Associates, Inc., Sunderland, MA. 607 pp.
- Kass, R.S., and M.C. Sanguinetti. 1984. Inactivation of calcium channel current in the calf cardiac Purkinje fiber: evidence for voltage- and calcium-mediated mechanisms. *J. Gen. Physiol.* 84:705–726.
- Lacerda, A.E., H.S. Kim, P. Ruth, E. Perez-Reyes, V. Flockerzi, F. Hofmann, L. Birnbaumer, and A.M. Brown. 1991. Normalization of current kinetics by interaction between the α_1 and β subunits of the skeletal muscle dihydropyridine-sensitive Ca^{2+} channel. *Nature*. 352:527–530.
- Lorenzon, N.M., M. Grabner, and K.G. Beam. 1999. N-terminal tagging of the skeletal ryanodine receptor with green fluorescent protein does not interfere with the restoration of bi-directional coupling. *Biophys. J.* 76:A304. (Abstr.)
- McPherson, P.S., and K.P. Campbell. 1993. The ryanodine receptor/ Ca^{2+} release channel. *J. Biol. Chem.* 268:13765–13768.
- Mikami, A., K. Imoto, T. Tanabe, T. Niidome, Y. Mori, H. Takeshima, S. Narumiya, and S. Numa. 1989. Primary structure and functional expression of the cardiac dihydropyridine-sensitive calcium channel. *Nature*. 340:230–233.
- Nabauer, M., G. Callewaert, L. Cleemann, and M. Morad. 1989. Regulation of calcium release is gated by calcium current, not gating charge, in cardiac myocytes. *Science*. 244:800–803.
- Nakai, J., R.T. Dirksen, H.T. Nguyen, I.N. Pessah, K.G. Beam, and P.D. Allen. 1996. Enhanced dihydropyridine receptor channel activity in the presence of ryanodine receptor. *Nature*. 380:72–75.
- Nakai, J., T. Ogura, F. Protasi, C. Franzini-Armstrong, P.D. Allen, and K.G. Beam. 1997. Functional nonequality of the cardiac and skeletal ryanodine receptors. *Proc. Natl. Acad. Sci. USA.* 94:1019–1022.
- Nakai, J., N. Sekiguchi, T.A. Rando, P.D. Allen, and K.G. Beam. 1998b. Two regions of the ryanodine receptor involved in coupling with L-type Ca^{2+} channels. *J. Biol. Chem.* 273:13403–13406.
- Nakai, J., T. Tanabe, T. Konno, B. Adams, and K.G. Beam. 1998a. Localization in the II-III loop of the dihydropyridine receptor of a sequence critical for excitation-contraction coupling. *J. Biol. Chem.* 273:24983–24986.
- Neely, A., X. Wei, R. Olcese, L. Birnbaumer, and E. Stefani. 1993. Potentiation by the β subunit of the ratio of the ionic current to the charge movement in the cardiac calcium channel. *Science*. 262:575–578.
- O'Connell, K.M.S., and R.T. Dirksen. 2000. Prolonged depolarization accelerates activation of the L-type Ca^{2+} current (L-current) in mouse skeletal myotubes. *Biophys. J.* 78:370a. (Abstr.)
- Peterson, B.Z., C.D. DeMaria, and D.T. Yue. 1999. Calmodulin is the Ca^{2+} sensor for Ca^{2+} -dependent inactivation of L-type calcium channels. *Neuron*. 22:549–558.
- Ríos, E., and G. Brum. 1987. Involvement of dihydropyridine receptors in excitation-contraction coupling in skeletal muscle. *Nature*. 325:717–720.
- Schneider, M.F., and W.K. Chandler. 1973. Voltage-dependent charge movement of skeletal muscle: a possible step in excitation-contraction coupling. *Nature*. 242:244–246.
- Singer, D., M. Biel, I. Lotan, V. Flockerzi, F. Hofmann, and N. Dascal. 1991. The roles of the subunits in the function of the calcium channel. *Science*. 253:1553–1557.
- Shistik, E., T. Ivanina, T. Puri, M. Hosey, and N. Dascal. 1995. Ca^{2+} current enhancement by α_2/δ and β subunits in *Xenopus* oocytes: contributions of changes in channel gating and α_1 protein level. *J. Physiol.* 489:55–62.
- Strube, C., M. Beurg, P.A. Powers, R.G. Gregg, and R. Coronado. 1996. Reduced Ca^{2+} current, charge movement, and absence of Ca^{2+} transients in skeletal muscle deficient in dihydropyridine receptor β_1 subunit. *Biophys. J.* 71:2531–2543.
- Strube, C., M. Beurg, M. Sukhareva, C.A. Ahern, J.A. Powell, P.A. Powers, R.G. Gregg, and R. Coronado. 1998. Molecular origin of the L-type Ca^{2+} current of skeletal muscle myotubes selectively deficient in dihydropyridine receptor β_{1a} subunit. *Biophys. J.* 75:207–217.
- Takekura, H., and C. Franzini-Armstrong. 1999. Correct targeting of dihydropyridine receptors and triadin in dyspedic mouse skeletal muscle in vivo. *Dev. Dyn.* 214:372–380.
- Takekura, H., M. Nishi, T. Noda, H. Takeshima, and C. Franzini-Armstrong. 1995. Abnormal junctions between surface membrane and sarcoplasmic reticulum in skeletal muscle with a mutation targeted to the ryanodine receptor. *Proc. Natl. Acad. Sci. USA.* 92:3381–3385.
- Takeshima, H., M. Iino, H. Takekura, M. Nishi, J. Kuno, O. Minowa, H. Takano, and T. Noda. 1994. Excitation-contraction uncoupling and muscular degeneration in mice lacking functional skeletal muscle ryanodine-receptor gene. *Nature*. 369:556–559.
- Tanabe, T., B.A. Adams, S. Numa, and K.G. Beam. 1991. Repeat I of the dihydropyridine receptor is critical in determining calcium channel activation kinetics. *Nature*. 352:800–803.
- Tanabe, T., K.G. Beam, B.A. Adams, T. Niidome, and S. Numa. 1990. Regions of the skeletal muscle dihydropyridine receptor critical for excitation-contraction coupling. *Nature*. 346:567–569.
- Tanabe, T., K.G. Beam, J.A. Powell, and S. Numa. 1988. Restoration of excitation-contraction coupling and slow calcium current in dysgenic muscle by dihydropyridine receptor complementary DNA. *Nature*. 336:134–139.
- Varadi, G., P. Lory, D. Schultz, M. Varadi, and A. Schwartz. 1991. Acceleration of activation and inactivation by the β subunit of the skeletal muscle calcium channel. *Nature*. 352:159–162.
- Wei, X., E. Perez-Reyes, A.E. Lacerda, G. Schuster, A.M. Brown, and L. Birnbaumer. 1991. Heterologous regulation of the cardiac calcium channel α_1 subunit by skeletal muscle β and γ subunits. *J. Biol. Chem.* 266:21943–21947.